## Title

Small molecule inhibition of IRE1α kinase/RNase has anti-fibrotic effects in the lung



## Journal

PLOS ONE, 14(1)

## ISSN

1932-6203

## Authors

Thamsen, Maike
Ghosh, Rajarshi
Auyeung, Vincent C
et al.

## Publication Date

2019

## DOI

10.1371/journal.pone.0209824

PLOS ONE

RESEARCH ARTICLE

# Small molecule inhibition of IRE1α kinase/RNase has anti-fibrotic effects in the lung

**Maike Thamsen[1,2,3,4], Rajarshi Ghosh[1,2,3,4], Vincent C. Auyeung[1,4,5], Alexis Brumwell[1,5,6], Harold A. Chapman[1,5,6], Bradley J. Backes[1,2,4], Gayani Perara[7], Dustin J. Maly[7], Dean Sheppard[1,4,5], Feroz R. Papa[1,2,3,4,8]***

**1** Department of Medicine, University of California, San Francisco, California, United States of America, **2** Diabetes Center, University of California, San Francisco, California, United States of America, **3** Quantitative Biosciences Institute (QBI), University of California, San Francisco, California, United States of America, **4** Lung Biology Center, University of California, San Francisco, California, United States of America, **5** Division of Pulmonary, Critical Care, Allergy, and Sleep Medicine, University of California, San Francisco, California, United States of America, **6** Cardiovascular Research Institute, University of California, San Francisco, California, United States of America, **7** Department of Chemistry and Department of Biochemistry, University of Washington, Seattle, Washington, United States of America, **8** Department of Pathology, University of California, San Francisco, California, United States of America

* frpapa@medicine.ucsf.edu





**Citation:** Thamsen M, Ghosh R, Auyeung VC, Brumwell A, Chapman HA, Backes BJ, et al. (2019) Small molecule inhibition of IRE1α kinase/RNase has anti-fibrotic effects in the lung. PLoS ONE 14 (1): e0209824. https://doi.org/10.1371/journal.pone.0209824

**Editor:** Michael Koval, Emory University School of Medicine, UNITED STATES

**Received:** August 23, 2018

**Accepted:** December 12, 2018

**Published:** January 9, 2019



**Data Availability Statement:** All relevant data are within the paper and its Supporting Information files.

**Funding:** This work was supported by P01 HL108794 from the National Heart Lung and Blood Institute to F.R.P. and D.S.. V.C.A. was supported by the UCSF Multidisciplinary Training Program in Lung Disease (5T32 HL007185 from the National Heart Lung and Blood Institute). The funders had no role in study design, data collection and

## Abstract

Endoplasmic reticulum stress (ER stress) has been implicated in the pathogenesis of idiopathic pulmonary fibrosis (IPF), a disease of progressive fibrosis and respiratory failure. ER stress activates a signaling pathway called the unfolded protein response (UPR) that either restores homeostasis or promotes apoptosis. The bifunctional kinase/RNase IRE1α is a UPR sensor/effector that promotes apoptosis if ER stress remains high and irremediable (i.e., a "terminal" UPR). Using multiple small molecule inhibitors against IRE1α, we show that ER stress-induced apoptosis of murine alveolar epithelial cells can be mitigated in vitro. In vivo, we show that bleomycin exposure to murine lungs causes early ER stress to activate IRE1α and the terminal UPR prior to development of pulmonary fibrosis. Small-molecule IRE1α kinase-inhibiting RNase attenuators (KIRAs) that we developed were used to evaluate the contribution of IRE1α activation to bleomycin-induced pulmonary fibrosis. One such KIRA—KIRA7—provided systemically to mice at the time of bleomycin exposure decreases terminal UPR signaling and prevents lung fibrosis. Administration of KIRA7 14 days after bleomycin exposure even promoted the reversal of established fibrosis. Finally, we show that KIRA8, a nanomolar-potent, monoselective KIRA compound derived from a completely different scaffold than KIRA7, likewise promoted reversal of established fibrosis. These results demonstrate that IRE1α may be a promising target in pulmonary fibrosis and that kinase inhibitors of IRE1α may eventually be developed into efficacious anti-fibrotic drugs.

## Introduction

The unfolded protein response (UPR) is a conserved intracellular signaling pathway that is activated when eukaryotic cells experience protein folding stress in the endoplasmic reticulum

analysis, decision to publish, or preparation of the manuscript.

**Competing interests:** The authors have declared that no competing interests exist.

(i.e., ER stress). The mammalian UPR is mediated by three sensors of unfolded protein situated in the ER membrane: IRE1α, ATF6, and PERK; of these, IRE1α is the most ancient member as IRE1 orthologs are present in all eukaryotes [1].

Depending on the severity of ER stress, the activity of IRE1α determines cell fate outcomes. When ER stress is remediable, IRE1α homodimerizes in the ER membrane, causing *trans*-autophosphorylation and selective activation of its C-terminal RNase domain to catalyze frame-shift splicing of the mRNA encoding the transcription factor XBP1 into its active form (i.e., XBP1s transcription factor) [2–4]. XBP1s in turn promotes homeostasis by upregulating the transcription of many components of the ER protein folding machinery including chaperones and post-translational modification enzymes [5,6]. If these adaptive outputs fail to resolve ER stress, IRE1α continues to self-associate into higher-order oligomers in the ER membrane, resulting in kinase hyperphosphorylation and consequent RNase hyperactivation [7,8]. Hyperactivated IRE1α RNase catalyzes endonucleolytic degradation of many messenger RNAs that localize to the ER membrane [7,9]. Hyperactivated IRE1α also cleaves and degrades the precursor of the microRNA, miR-17, which in turn relieves gene repression of thioredoxin-interacting protein (TXNIP). This pathway culminates in apoptosis and is thus called the "terminal UPR" [10]; terminal UPR signaling underlies several diseases of premature cell loss [11].

Recent studies have implicated the UPR in the pathophysiology of human idiopathic pulmonary fibrosis (IPF), a disease of progressive interstitial fibrosis, which leads to severe debilitation and eventually respiratory failure and death [12]. Upregulation of the UPR occurs in both familial IPF and sporadic (non-familial) IPF. In one family, a missense mutation in Surfactant Protein C (SFTPC) causes misfolding of this variant protein and consequent ER stress in alveolar epithelial cells [13,14], which is recapitulated in a mouse model bearing the same mutation [15]. In types 1 and 4 of the Hermansky-Pudlak syndrome, patients have homozygous loss-of-function at the *HPS1* or *HPS4* loci and develop a devastating pulmonary fibrosis virtually indistinguishable from IPF by early adulthood [16]. *HPS1* or *HPS4* loss-of-function causes accumulation of immature surfactant protein in alveolar epithelial cells and consequently ER stress and apoptosis [17]. Activation of the UPR has also been demonstrated in patients with non-familial (sporadic) IPF [18,19], although the trigger for UPR activation in these patients is unclear. It has been suggested that environmental toxins (cigarette smoke) and infectious agents (e.g. herpesviruses) may increase the secretory workload of alveolar epithelial cells, which may exhaust homeostatic UPR signaling and ultimately trigger the terminal UPR and cell death [19–21]. In mice, the chemical ER stress inducer tunicamycin is not sufficient to induce fibrosis, but exacerbates fibrosis in the presence of another injury in the form of bleomycin [15]. Administration of the nonspecific "chemical chaperones" 4-PBA or TUDCA mitigated fibrosis after bleomycin injury [22].

Together, these findings suggest that dampening UPR signaling, perhaps through inhibiting IRE1α, might provide therapeutic benefit in IPF. To these ends, our groups have developed small-molecule compounds that inhibit the IRE1α kinase and thereby allosterically regulate its RNase activity [23–25]. These kinase-inhibiting RNase attenuating (KIRA) compounds dose-dependently reduce IRE1α's destructive UPR signaling and thereby spare cells experiencing unrelieved ER stress [8,26].

Here we show that ER stress induces apoptosis in a mouse alveolar epithelial cell line and mouse primary type II alveolar epithelial cells, and that inhibiting the IRE1α RNase mitigates apoptosis in vitro. We further show that ER stress and stereotypic terminal UPR signature changes occur early in mouse models of bleomycin-induced pulmonary fibrosis, and that administration of a KIRA compound at the time of bleomycin exposure prevents the full fibrosis phenotype. Importantly, we show that KIRA compounds are efficacious even when

administered *after* the onset of fibrosis. These studies suggest the possible benefit of the KIRA class of compounds in human IPF.

## Results

### ER stress-induced apoptosis in alveolar epithelial cells depends on IRE1α activity

Severe or persistent ER stress has been shown to induce apoptosis in diverse cell types [11]. Since chronic epithelial injury is thought to underlie both familial and sporadic IPF, we assessed whether ER stress induces apoptosis in alveolar epithelial cells. The mouse epithelial cell line MLE12 was exposed to tunicamycin, which inhibits N-linked protein glycosylation and induces protein misfolding in the endoplasmic reticulum. Tunicamycin induced robust splicing of XBP1 mRNA in MLE12 cells, which was dose-dependently inhibited by provision of the covalent IRE1α RNase inhibitor STF-083010 [27] (Fig 1A). Low doses of tunicamycin (30 ng/ml) were sufficient to induce apoptosis in MLE12 cells as measured by annexin V expression (Fig 1B). Tunicamycin-induced apoptosis depended on IRE1α RNase activity, since STF-083010 promoted cell survival. Next, we isolated primary type II alveolar epithelial cells from mouse lungs by dissociation and cell sorting as previously described [28,29]. As in the MLE12 cell lines, tunicamycin induced apoptosis in primary type II alveolar epithelial cells; apoptosis again depended on IRE1α, since administration of the IRE1α RNase inhibitor STF-083010 promoted cell survival in the presence of tunicamycin (Fig 1C).

### ER stress precedes fibrosis in the bleomycin model pulmonary fibrosis

To evaluate the role of IRE1α in vivo, we turned to the bleomycin model of pulmonary fibrosis. C57/BL6 mice were exposed to a single dose of intranasal bleomycin (1.5 units/kg), and whole lung RNA was collected at intervals after exposure. Total XBP1 mRNA levels rise within 2 days of bleomycin exposure ($p<0.01$), followed by markers of terminal UPR activation: the chaperone BiP ($p<0.001$), and the transcription factors ATF4 ($p<0.01$) and CHOP ($p<0.05$) (Fig 2A). This wave of ER stress and terminal UPR activation peaks at day 8 and remains elevated through day 26 (Fig 2A). This initial, early wave of terminal UPR signaling was followed by

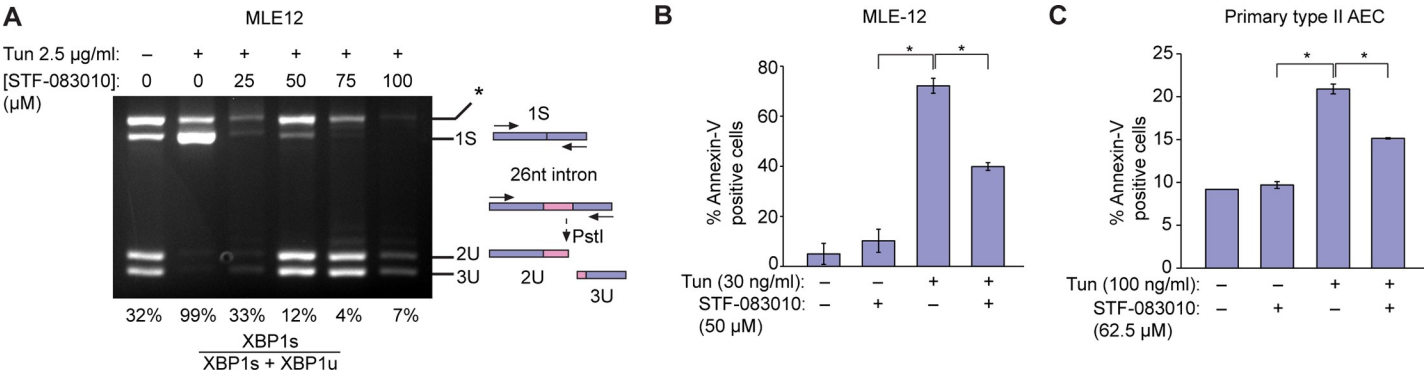


**Fig 1. ER stress activates IRE1α to induce apoptosis in alveolar epithelial cells.** (A) Ethidium bromide-stained agarose gel of XBP1 cDNA amplicons. Mouse Lung Epithelial (MLE12) cells were exposed to Tunicamycin (Tun) 2.5 μg/ml and indicated concentrations of STF-083010 for 4 hrs. The cDNA amplicon of unspliced XBP1 mRNA is cleaved by a PstI site within a 26 nucleotide intron to give 2U and 3U. IRE1α-mediated cleavage of the intron and re-ligation *in vivo* removes the PstI site to give the 1S (spliced) amplicon. * denotes a spliced/unspliced XBP1 hybrid amplicon. The ratio of spliced over (spliced + unspliced) amplicons—1S/(1S+2U+3U)—is reported as %XBP1 splicing under the respective lanes. (B) Percent MLE12 cells staining positive for Annexin V after treatment with Tm (30 ng/ml) and STF-083010 (50 μM) for 72 hrs. (C) Percent primary mouse alveolar epithelial cells (AEC) staining positive for Annexin V after treatment with Tm (100 ng/ml) and STF-083010 (62.5 μM) for 72 hrs. Three independent biological samples were used for Annexin V staining experiments. Data are means +/- SD. P value: * <0.05.

https://doi.org/10.1371/journal.pone.0209824.g001

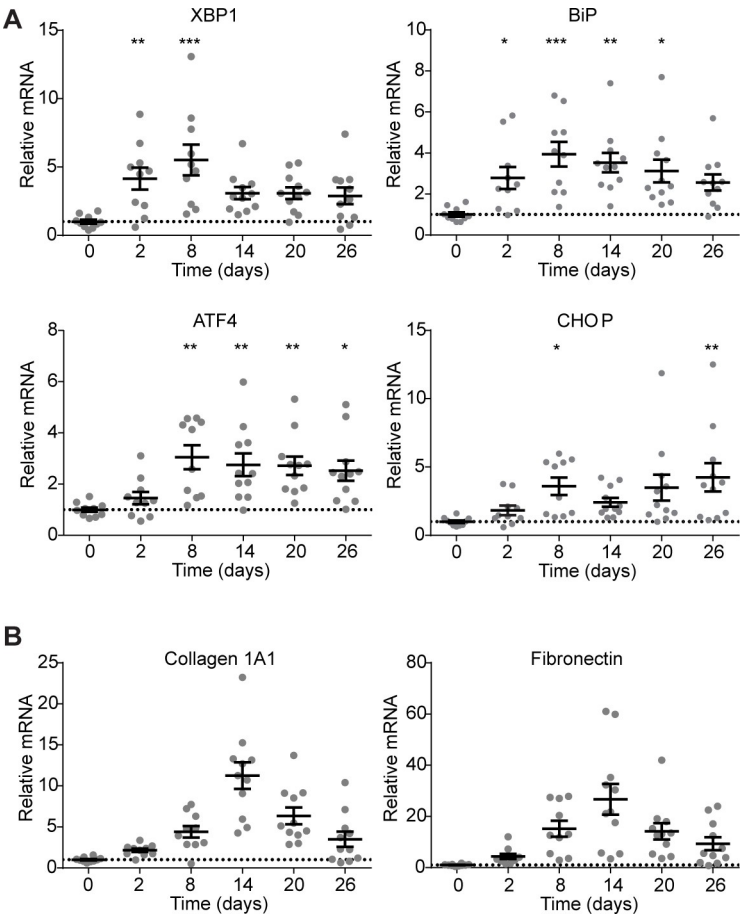


**Fig 2. ER stress and terminal UPR signaling precede fibrosis in bleomycin-exposed mice.** (A) Quantitative PCR of UPR markers XBP1, BiP, ATF4, and CHOP from mice at 0, 2, 8, 14, 20, or 26 days after a single exposure to bleomycin. Each mouse is represented by a dot, and whiskers denote group mean +/- SEM. (B) Quantitative PCR for collagen 1A1 mRNA and fibronectin mRNA from at 0, 2, 8, 14, 20, or 26 days after a single exposure to bleomycin. Each mouse is represented by a dot, and whiskers denote group mean +/- SEM. P values: $^{*}<0.05$, $^{**}<0.01$, $^{***}<0.001$.

https://doi.org/10.1371/journal.pone.0209824.g002

overt fibrosis; mRNA levels of collagen 1A1 and fibronectin rose at day 8 and peaked on day 14, followed by waning levels over the following two weeks (Fig 2B).

We stained formalin-fixed, paraffin-embedded sections of lungs from mice exposed to saline or bleomycin for XBP1 to ascertain whether the UPR hyperactivation occurred in a discrete population of cells. XBP1 stained most prominently in bronchial epithelial cells in saline-exposed mice; after bleomycin exposure, XBP1 staining occurred diffusely throughout the lung (S1 Fig). Thus, multiple cell types contribute to the observed upregulation in terminal UPR markers after bleomycin exposure.

## KIRA7 modulation of IRE1α prevents bleomycin-induced fibrosis

The timing of ER stress and terminal UPR activation compared to fibrosis onset suggested that pharmacologic blockade of UPR pathways during the period shortly after bleomycin exposure might mitigate bleomycin-induced fibrosis. Because chronic epithelial injury and apoptosis is thought to underlie IPF [30], we focused on the PERK and IRE1α pathways. These endoplasmic reticulum resident sensors are known to induce apoptosis through a variety of mechanisms, including PERK activating the pro-apoptotic transcription factor CHOP, and

hyperactivation of IRE1α leading to activation of JNK,the NLRP3 inflammasome, and consequent caspase cleavage [1]. These pathways are not mutually exclusive, and in fact can be mutually reinforcing; for example, IRE1α overexpression alone is sufficient by itself to induce CHOP [9].

We first evaluated the IRE1α pathway. The RNase inhibitor STF-083010 is a poor tool compound for in vivo use in part due to its high $IC_{50}$ of 25 μM and poor solubility (Selleckchem manufacturer datasheet; [27]). Therefore, for in vivo experiments we used KIRA7, an imidazopyrazine compound that binds the IRE1α kinase to allosterically inhibit its RNase activity (Fig 3A). KIRA7, also referred to a Compound 13 [25], is a modification of our previously published compound KIRA6 [8] with comparable potency, and pharmacokinetic properties including bioavailability. Mice were exposed to a single dose of intranasal bleomycin (1.5 units/kg), then treated with either KIRA7 (5 mg/kg/day i.p.) or an equivalent volume of vehicle, starting on the day of bleomycin exposure and continuing daily for 14 days. Whole lung protein and RNA were collected on day 14 for analysis (Fig 3B).

Although day 14 is after peak expression of markers of the terminal UPR (Fig 2A), protein levels of spliced XBP1 and ATF4 remain significantly elevated in bleomycin-exposed mice, compared to saline-exposed controls (Fig 3C). Treatment of bleomycin-exposed mice with KIRA7 resulted in decreased spliced XBP1 and ATF4, compared to bleomycin exposed mice treated with vehicle (Fig 3C). Likewise, mRNA levels of BiP and CHOP are significantly elevated after bleomycin exposure, and treatment of bleomycin-exposed mice with KIRA7 decreased these levels (Fig 3D, $p<0.05$).

These decreases in markers of the terminal UPR were accompanied by significant improvements in bleomycin-induced fibrosis. Histologically, bleomycin exposure induced destruction of alveoli, cell infiltration, and architectural distortion in the lung. In contrast, alveolar architecture was largely preserved in lungs of mice exposed to bleomycin and treated with KIRA7 (Fig 3E). Picrosirius red staining for birefringent mature collagen fibrils [31] (Fig 3F) revealed significant decreases in the area of fibrosis in mice preventively treated with KIRA7 (Fig 3G, $p<0.05$). Bleomycin exposure increased total hydroxyproline, a quantitative measure of collagen content, and total lung weight; and both were significantly decreased with KIRA7 treatment ($p<0.05$). Consistent with these decreases, mRNA levels of collagen 1A1 and fibronectin were both significantly decreased by KIRA7 treatment ($p<0.001$ and $p<0.01$, respectively).

We also evaluated the contribution of the PERK pathway to fibrosis development in the bleomycin model using the PERK kinase inhibitor GSK2606414 [32]. Mice were exposed to a single dose of intranasal bleomycin (1.5 units/kg), then treated with either GSK2606414 (50 mg/kg/day i.p.) or an equivalent volume of vehicle, starting on the day of bleomycin exposure and continuing daily for 14 days (S2 Fig, Panel A). This dose of GSK2606414 had previously been shown to be sufficient to protect mice from prion-induced neurodegeneration, and causes mild hyperglycemia [33]. Demonstrating target engagement, GSK2606414 treatment decreased whole lung ratios of phospho-eIF2α to total eIF2α, the endogenous PERK kinase substrate (S2 Fig, Panel B). GSK2606414 treatment induced hyperglycemia (S2 Fig, Panel C), as expected. However, GSK2606414 did not decrease fibrosis as measured by lung hydroxyproline content (S2 Fig, Panel D).

## KIRA7 modulation of IRE1α mitigates established fibrosis

Administration of KIRA7 protects against fibrosis during the initial injury after bleomycin, which is also when ER stress and terminal UPR markers are at their peak (Fig 2A). We wondered whether KIRA7 might even protect against fibrosis when administered later (i.e., in a therapeutic rather than a prophylactic regimen), two weeks after initial injury, when terminal

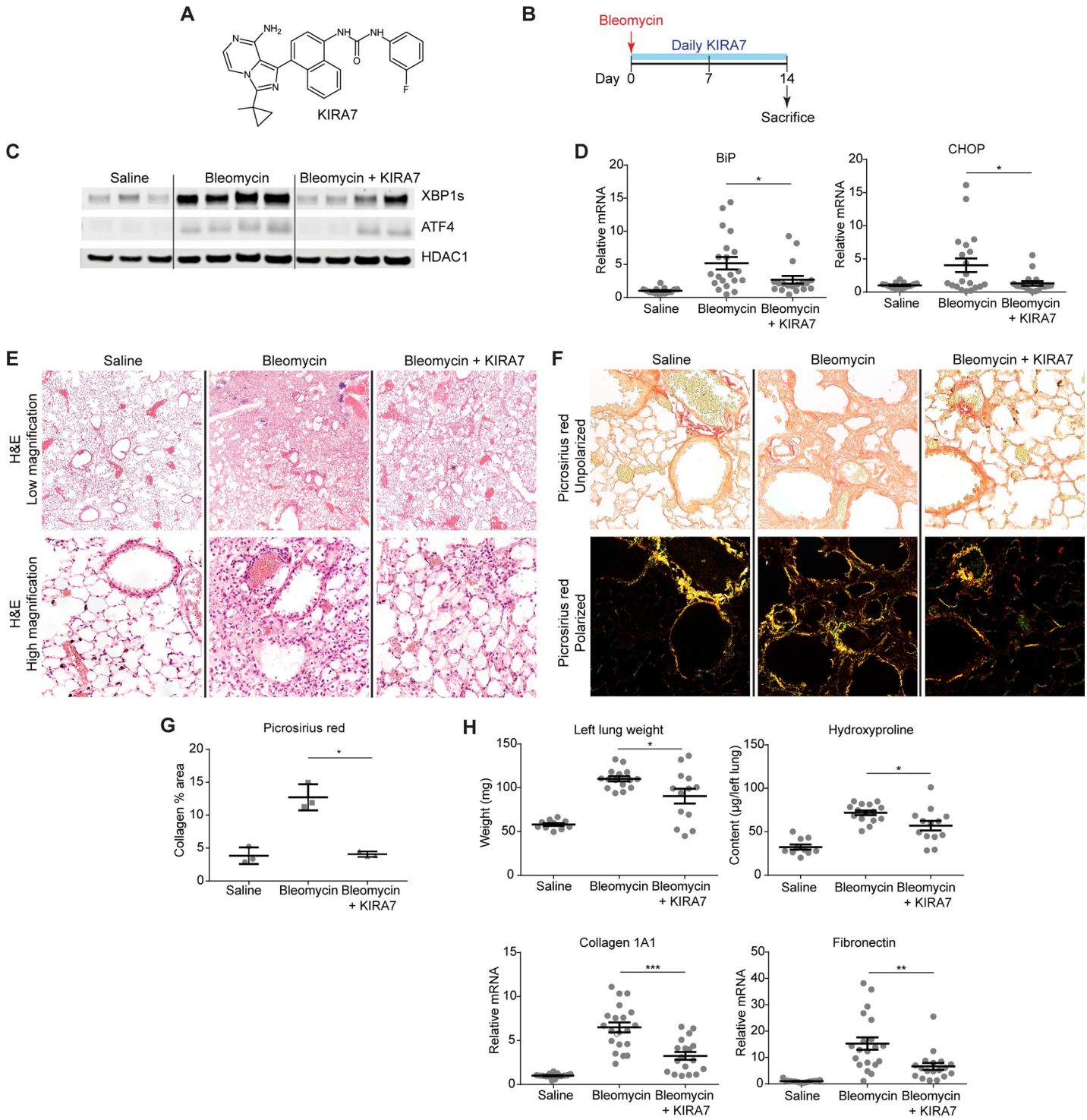


**Fig 3. KIRA7 prevents bleomycin-induced fibrosis.** (A) Chemical structure of KIRA7. (B) Schematic of the KIRA7 prevention regimen. Mice were exposed to saline or bleomycin once, then treated with KIRA7 or vehicle beginning from the time of bleomycin exposure and daily for two weeks after exposure. (C) Western blot of terminal UPR transcription factors XBP1s and ATF4 from mice treated according to the prevention regimen. (D) Quantitative PCR of terminal UPR markers BiP and CHOP from mice treated according to the prevention regimen. Each mouse is represented by a dot, and whiskers denote group mean +/- SEM. (E) Hematoxylin and eosin stained sections from mice treated according to the prevention regimen, at low magnification (top) and high magnification (bottom). (F) Representative high-magnification sections stained with picrosirius red, from mice treated as in (E), under unpolarized (top) and polarized light (bottom). (G) Quantification of picrosirius red stained fibrillar collagen from (F). Each mouse is represented by a dot and whiskers denote group mean +/- SEM. (H) Markers of fibrosis (lung weight, hydroxyproline content, collagen 1A1 mRNA, and fibronectin mRNA) from mice treated according to the prevention regimen. Each mouse is represented by a dot, and whiskers denote group mean +/- SEM. P values: $^{*}<0.05$, $^{**}<0.01$, $^{***}<0.001$.

https://doi.org/10.1371/journal.pone.0209824.g003

UPR markers are still elevated albeit to a lesser degree (Fig 2A). In addition, early injury in the first week after bleomycin administration is characterized by neutrophilic and lymphocytic inflammatory infiltration, which is not thought to be characteristic of human IPF [34]. The initial alveolitis clears around day 7, followed by fibroblast proliferation and matrix deposition; fibrosis is typically established by day 14 (Fig 2B) [34]. Thus, administration of KIRA7 after day 14 may have greater relevance to human IPF, where fibrosis may progress for years before the onset of clinical symptoms and diagnosis.

As before, mice were exposed to a single dose of intranasal bleomycin (1.5 units/kg). Beginning on day 14, mice were treated with either KIRA7 (5 mg/kg/day i.p.) or an equivalent volume of vehicle; injections were continued daily until day 28. Whole lung protein and RNA were collected on day 28 for analysis (Fig 4A). As expected, bleomycin-exposed mice had increased levels of spliced XBP1, ATF4, and CHOP protein at day 28 (Fig 4B). Treatment of bleomycin-exposed mice was associated with decreases in levels of these proteins (Fig 4B). KIRA7 also blunted bleomycin-induced increases in lung weight ($p<0.001$) and hydroxyproline ($p<0.05$) (Fig 4C). At day 28, mRNA levels of collagen 1A1 and fibronectin remain elevated above baseline, albeit at lower levels compared to day 28 (Fig 4C), consistent with the observation that synthesis of collagen and fibronectin mRNA peaks at day 14 and wanes thereafter (Fig 2B). Nonetheless, administration of KIRA7 decreased mRNA levels of collagen 1A1 ($p<0.05$) and fibronectin ($p<0.05$).

## KIRA8 modulation of IRE1α mitigates established fibrosis

A sulfonamide compound was recently described that is structurally unrelated to KIRA7 [35], but possesses the properties of an IRE1α kinase-inhibiting RNase attenuator, which we therefore call KIRA8 (Fig 5A). It has exceptional selectivity for IRE1α in whole-kinome testing, having little activity even against its closely related paralog IRE1β [26]. KIRA8 is highly potent against the IRE1α kinase ($IC_{50}$ = 5.9 nM, [26]), nearly 10-fold more potent than KIRA7 ($IC_{50}$ = 110 nM, [25]). Consistent with this, KIRA8 has higher potency than KIRA7 in inhibiting XBP1 splicing in the alveolar epithelial cell line MLE12 (Fig 5B).

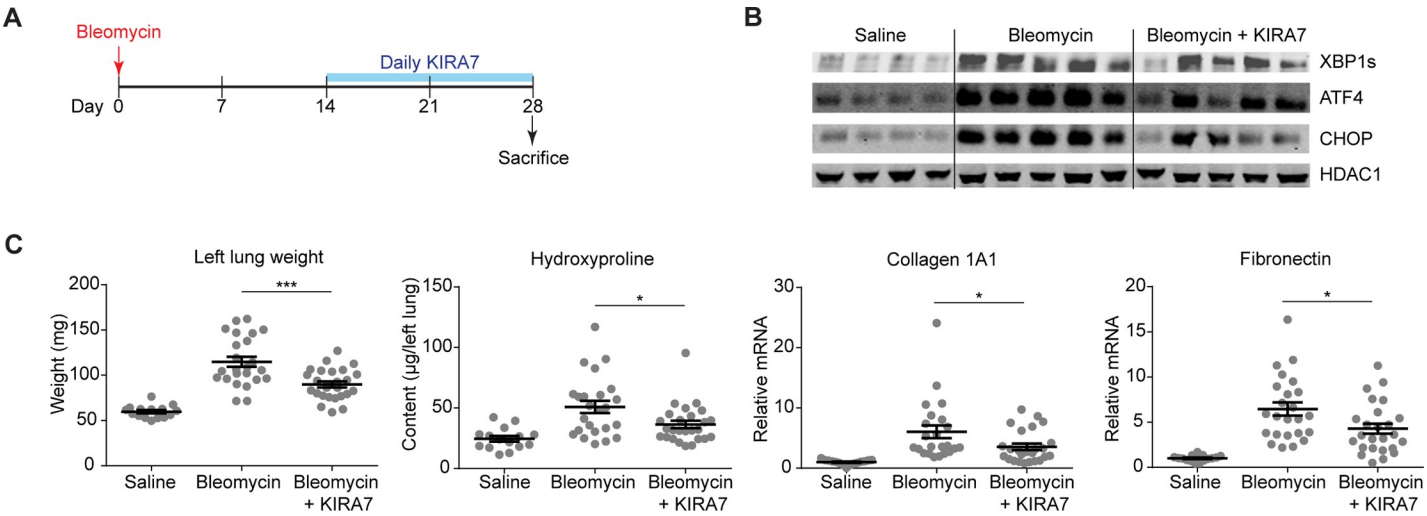


**Fig 4. KIRA7 reverses bleomycin-induced fibrosis when given 2 weeks after bleomycin exposure.** (A) Schematic of the KIRA7 reversal regimen. Mice were exposed to saline or bleomycin once, then treated with KIRA7 or vehicle beginning two weeks after bleomycin exposure and continuing daily for two additional weeks. (B) Western blot of terminal UPR transcription factors XBP1s, ATF4, and CHOP from mice treated with KIRA7 according to the reversal regimen. (C) Markers of fibrosis (lung weight, hydroxyproline content, collagen 1A1 mRNA, and fibronectin mRNA) from mice exposed to saline or bleomycin, and treated with KIRA7 according to the reversal regimen. Each mouse is represented by a dot, and whiskers denote group mean +/- SEM. P values: $^{*}<0.05$, $^{**}<0.01$, $^{***}<0.001$.

https://doi.org/10.1371/journal.pone.0209824.g004

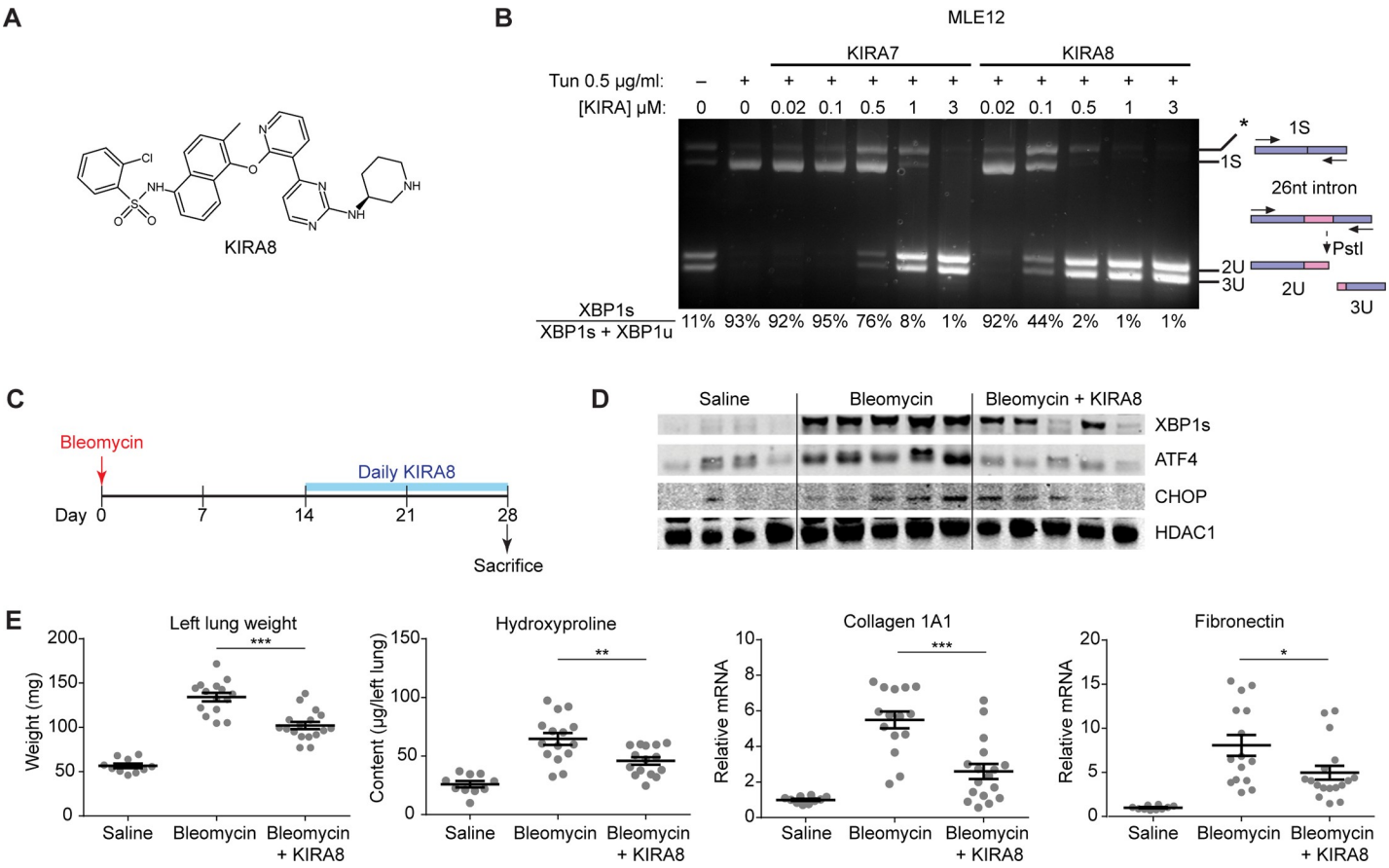


**Fig 5. KIRA8 reverses bleomycin-induced fibrosis when given 2 weeks after bleomycin exposure.** (A) Chemical structure of KIRA8. (B) Ethidium bromide-stained agarose gel of XBP1 cDNA amplicons after induction by treating Mouse Lung Epithelial (MLE12) cells with Tunicamycin (Tun) 0.5 μg/ml and indicated concentrations of KIRA7 or KIRA8 for 8 hrs. The ratio of spliced over (spliced + unspliced) amplicons—1S/(1S+2U+3U)—is reported as % XBP1 splicing and reported under respective lanes. (C) Schematic of the KIRA8 reversal regimen. Mice were exposed to saline or bleomycin once, then treated with KIRA8 or vehicle beginning two weeks after bleomycin exposure and continuing daily for two additional weeks. (D) Western blot of terminal UPR transcription factors XBP1s, ATF4, and CHOP from mice treated with KIRA8 according to the reversal regimen. (E) Markers of fibrosis (lung weight, hydroxyproline content, collagen 1A1 mRNA, and fibronectin mRNA) from mice exposed to saline or bleomycin, and treated with KIRA8 according to the reversal regimen. Each mouse is represented by a dot, and whiskers denote group mean +/- SEM. P values: $^{*}<0.05$, $^{**}<0.01$, $^{***}<0.001$.

https://doi.org/10.1371/journal.pone.0209824.g005

We evaluated the ability of KIRA8 to mitigate established fibrosis. Mice were exposed to a single dose of intranasal bleomycin (1.5 units/kg), and treated with either KIRA8 (50 mg/kg/day i.p.) or an equivalent volume of vehicle starting at day 14 and continuing daily until day 28. Whole lung protein and RNA were collected on day 28 for analysis (Fig 5C). KIRA8 treated mice had lower levels of spliced XBP1, ATF4, and CHOP protein (Fig 5D). As before, KIRA8 treatment attenuated bleomycin-induced increases in lung weight ($p<0.001$) and hydroxyproline ($p<0.01$), and decreased mRNA expression of collagen 1A1 ($p<0.001$) and fibronectin ($p<0.05$) (Fig 5E).

## Discussion

We have shown that ER stress induces apoptosis in a mouse alveolar epithelial cell line and mouse primary type II alveolar epithelial cells, and that inhibiting the IRE1α RNase mitigates apoptosis in vitro. *In vivo*, bleomycin exposure to the mouse lung induces ER stress prior to the onset of fibrosis in multiple cell types. Highlighting the importance of ER stress and IRE1α

in this model, administration of KIRA7 starting from the time of bleomycin exposure decreased markers of ER stress and prevented fibrosis. Importantly, KIRA7 was efficacious even when administered two weeks after the onset of fibrosis. KIRA8 is a next-generation KIRA compound derived from a completely different scaffold than KIRA7, with nanomolar potency and monoselectivity for the IRE1α kinase. KIRA8 likewise promoted the reversal of established fibrosis.

In this work, we evaluated the IRE1α and PERK pathways because these arms of the UPR are best known to induce apoptosis under conditions of severe ER stress. These pathways are not mutually exclusive, and may be mutually reinforcing. For example, while this paper was under review, CHOP gene deletion was reported to protect mice from pulmonary fibrosis induced by repetitive bleomycin exposure and hypoxia [36]. Both PERK and IRE1α were independently required for hypoxia-induced CHOP expression in alveolar epithelial cell culture [36]. That study, and the observation that IRE1α overexpression is sufficient by itself to induce CHOP [9], highlight the significant cross-talk between the PERK and IRE1α pathways in vitro. In vivo, however, we found that PERK inhibition with GSK2606414 failed to prevent pulmonary fibrosis after bleomycin, while IRE1α inhibition with KIRA7 or KIRA8 both prevented and reversed fibrosis. Thus, our results support the relative, but not exclusive, importance of the IRE1α pathway in bleomycin-induced fibrosis.

Our work suggests that targeting IRE1α might be a promising therapeutic target to be tested clinically for human IPF. A prevailing view is that IPF is caused by chronic epithelial injury, which induces fibroblast activation and collagen deposition [30]. In some cases, heritable defects in cargo protein folding or post-translational processing leads to chronic ER stress, IRE1α activation, terminal UPR signaling, and epithelial cell apoptosis [13,14,16]. Others have proposed that various insults to the alveolar epithelium lead ultimately to terminal UPR signaling [18–21]. In both cases, modulating the activity of IRE1α would be predicted to blunt terminal UPR signaling, promote alveolar epithelial cell survival, and thus mitigate ongoing fibrosis.

Another intriguing possibility is that IRE1α activity may also contribute directly to pathologic fibroblast behavior. For example, in fibroblasts derived from patients with systemic sclerosis, IRE1α was required for TGFβ1-induced differentiation into activated myofibroblasts [37]. This finding may help explain why late administration of KIRA7 and KIRA8, two weeks after bleomycin injury, can promote the reversal of established fibrosis (Figs 4 and 5). The possible roles of IRE1α in epithelial cells and fibroblasts are not mutually exclusive, and extensive work outside the scope of this study is needed to elucidate the precise role(s) of IRE1α in the injured lung.

The anti-fibrotic activity of KIRA7 and KIRA8, even when administered late, is particularly important when considering potential therapeutic avenues in human disease. In IPF, subclinical fibrosis starts years before patients are symptomatic enough to come to medical attention, and even then diagnosis is often delayed [30,38]. These results suggest that targeting IRE1α may possibly be effective even when fibrosis is advanced. In addition, severe pathological lung fibrosis, evidenced by the "usual interstitial pneumonia" pattern radiographically and histologically, is the final common endpoint to chronic injury in non-IPF interstitial lung diseases, including connective tissue-associated interstitial lung disease, chronic hypersensitivity pneumonitis, and asbestosis [39]. Targeting IRE1α holds therapeutic promise to the extent that ER stress is important to the primary pathology and initial injury in these diseases, as has been suggested in some forms of genetic autoimmune-associated interstitial lung disease [40] and asbestosis [41]. To the extent that targeting IRE1α might directly mitigate pathological fibroblast activity, targeting IRE1α may be useful even in cases where ER stress is not part of the primary pathology.

In summary, we have shown that intra-airway bleomycin, the most commonly used murine model of pulmonary fibrosis, induces the unfolded protein response and that this response precedes the development of pulmonary fibrosis. Furthermore, two chemically distinct small molecules that inhibit IRE1α kinase and attenuate its RNase activity (KIRAs) are effective in preventing and reversing bleomycin induced pulmonary fibrosis. This work lays the groundwork for developing KIRAs as novel therapeutics for IPF and other interstitial lung diseases characterized by progressive pulmonary fibrosis.

## Materials and methods

### Tissue culture

Mouse Lung Epithelial (MLE12) cells were obtained from ATCC and grown in HITES media as formulated by ATCC. Tunicamycin (Tun) was purchased from Millipore. STF-083010, KIRA7 and KIRA8 were synthesized in house. Mouse primary AECII cells were isolated as described [42]. Cells were grown in SAGM media (Lonza CC-3118) on fibronectin coated plates.

### XBP1 mRNA splicing

RNA was isolated from whole cells or mouse tissues and reverse transcribed as above to obtain total cDNA. Then, XBP-1 primers were used to amplify an XBP-1 amplicon spanning the 26 nt intron from the cDNA samples in a regular 3-step PCR. Thermal cycles were: 5 min at 95˚C, 30 cycles of 30 s at 95˚C, 30 s at 60˚C, and 1 min at 72˚C, followed by 72˚C for 15 min, and a 4˚C hold. Mouse XBP1 sense (`5'-AGGAAACTGAAAAACAGAGTAGCAGC-3'`) and antisense (`5'-TCCTTCTGGGTAGACCTCTGG-3'`) primers were used. PCR fragments were then digested by PstI, resolved on 3% agarose gels, stained with EtBr and quantified by densitometry using NIH ImageJ.

### Annexin V apoptosis

Annexin V staining was used to quantify apoptosis by flow cytometry. Cells were plated in 12-well plates overnight and then treated with various reagents for indicated time periods. On the day of flow cytometry analysis, cells were trypsinized and washed in PBS and resuspended in Annexin V binding buffer with Annexin-V FITC (BD Pharmingen). Annexin V stained cells were counted using a Becton Dickinson LSRII flow cytometer.

### Bleomycin-induced pulmonary fibrosis

C57BL6 mice at 12 weeks of age were obtained from Jackson Laboratories. Mice were housed in specific pathogen-free conditions in the Animal Barrier Facility at the University of California, San Francisco. This work was approved by the Institutional Animal Care and Use Committee of the University of California, San Francisco. To induce fibrosis, mice were anesthetized with ketamine and xylazine and exposed to a single dose of intranasal bleomycin (1.5 units/kg). Mice were sacrificed by open-drop isoflurane overdose and lungs were harvested at the indicated times. For treatment, GSK2606414 was dissolved in a vehicle consisting of 2% DMSO, 20% (2-hydroxypropyl)-β-cyclodextrin, and 78% water and injected peritoneally at the indicated dosages and intervals. KIRA7 or KIRA8 was dissolved in a vehicle consisting of 3% ethanol, 7% Tween-80, and 90% normal saline and injected peritoneally at the indicated dosages and intervals.

Histological sections were prepared by inflating lungs with zinc formalin fixative, followed by paraffin embedding and sectioning. Picrosirius red (Abcam) staining was performed per

manufacturer's instructions. Quantification was performed on representative 4x-magnification fields imaged under polarized light, and the percent area covered by stained collagen measured using ImageJ software. Immunohistochemistry was performed with anti-XBP1 (Santa Cruz Biotechnology #7351, 1:200 dilution).

Lung hydroxyproline content was quantified by reaction with 4-(Dimethylamino)benzaldehyde reaction and colorimetry (Sigma). Messenger RNA levels were measured by reverse transcription and quantitative PCR as described below.

## RNA isolation and quantitative real-time PCR (qPCR)

A TissueLyser II (Qiagen) was used to homogenize mouse lungs for RNA isolation. RNA was isolated from lung homogenates or cultured cells using either Qiagen RNeasy kits or Trizol (Invitrogen). For cDNA synthesis, 1 μg total RNA was reverse transcribed using the QuantiTect Reverse Transcription Kit (Qiagen). For qPCR, we used SYBR green (Qiagen) and StepOnePlus Real-Time PCR System (Applied Biosystems). Thermal cycles were: 5 min at 95˚C, 40 cycles of 15 s at 95˚C, 30 s at 60˚C. Gene expression levels were normalized to 18S rRNA. Primers used for qPCR were as follows:

Human/Mouse 18S rRNA: 5′-GTAACCCGTTGAACCCCATT-3′ and 5′-CCATCCAATCGGTAGTAGCG-3′

Mouse XBP1: 5′-CCGTGAGTTTTCTCCCGTAA-3′ and 5′-AGAAAGAAAGCCCGGATGAG-3′

Mouse BiP: 5′-TCAGCATCAAGCAAGGATTG-3′ and 5′-AAGCCGTGGAGAAGATCTGA-3′

Mouse ATF4: 5′-GCAAGGAGGATGCCTTTTC-3′ and 5′-GTTTCCAGGTCATCCATTCG-3′

Mouse CHOP: 5′-CACATCCCAAAGCCCTCGCTCTC-3′ and 5′-TCATGCTTGGTGCAGGCTGACCAT-3′

Mouse Collagen 1A1: 5′-CCTGGTAAAGATGGTGCC-3′ and 5′-CACCAGGTTCACCTTTCGCACC-3′

Mouse Fibronectin: 5′-ACAGAAATGACCATTGAAGG-3′ and 5′-TGTCTGGAGAAAGGTTGATT-3′

## Western blot

Whole lungs were homogenized using a TissueLyzer II (Qiagen). Nuclear and cytoplasmic fractions were isolated using the NE-PER extraction kit (Thermo Fisher). Western blots were performed using 4%-12% Bis-Tris precast gels (Invitrogen) using MOPS buffer, then transferred onto nitrocellulose membranes. Antibody binding was detected using conjugated secondary antibodies (Li-Cor) on the Li-Cor Odyssey scanner. Antibodies used for Western blot were as follows: XBP1 (Biolegend 9D11A43), HDAC1 (Cell Signaling Technologies 5356), ATF4 (Sigma WH0000468M1), TXNIP (MBL International K0205-3), and CHOP (Cell Signaling Technologies 2895).

# Supporting information

**S1 Fig. Multiple cell types express XBP1 after bleomycin exposure.** Immunohistochemical staining in saline- and bleomycin-exposed mouse lungs, using rabbit IgG control and anti-

XBP1.
(TIF)

**S2 Fig. Failure of the PERK inhibitor GSK2606414 to mitigate bleomycin-induced fibrosis.** (A) Schematic of the GSK2606414 prevention regimen. Mice were exposed to saline or bleomycin once, then treated with GSK2606414 or vehicle beginning from the time of bleomycin exposure and daily for two weeks after exposure. (B) Western blot for phospho-eIF2α and total eIF2α from mice treated with GSK2606414 according to the reversal regimen (top) and quantification of phospho-eIF2α / total eIF2α ratio (bottom), normalized to saline-exposed lanes. (C) Blood glucose levels and (D) total hydroxyproline quantification from mice exposed to saline or bleomycin, and treated with GSK2606414 according to the reversal regimen. Each mouse is represented by a dot, and whiskers denote group mean +/- SEM. P values: $^{*}<0.05$, $^{**}<0.01$.
(TIF)

## Author Contributions

**Conceptualization:** Maike Thamsen, Rajarshi Ghosh, Dustin J. Maly, Dean Sheppard, Feroz R. Papa.

**Data curation:** Maike Thamsen, Rajarshi Ghosh, Alexis Brumwell, Harold A. Chapman, Gayani Perara.

**Formal analysis:** Maike Thamsen, Rajarshi Ghosh, Vincent C. Auyeung, Gayani Perara.

**Funding acquisition:** Dean Sheppard, Feroz R. Papa.

**Investigation:** Maike Thamsen, Rajarshi Ghosh, Vincent C. Auyeung, Alexis Brumwell, Bradley J. Backes, Gayani Perara.

**Methodology:** Maike Thamsen, Rajarshi Ghosh, Bradley J. Backes.

**Project administration:** Feroz R. Papa.

**Supervision:** Harold A. Chapman, Dustin J. Maly, Dean Sheppard, Feroz R. Papa.

**Writing – original draft:** Rajarshi Ghosh, Vincent C. Auyeung.

**Writing – review & editing:** Rajarshi Ghosh, Vincent C. Auyeung, Dean Sheppard, Feroz R. Papa.

## References

1. Hetz C, Papa FR. The Unfolded Protein Response and Cell Fate Control. Mol Cell. Elsevier Inc.; 2018; 69: 169–181. https://doi.org/10.1016/j.molcel.2017.06.017 PMID: 29107536
2. Yoshida H, Matsui T, Yamamoto A, Okada T, Mori K. XBP1 mRNA is induced by ATF6 and spliced by IRE1 in response to ER stress to produce a highly active transcription factor. Cell. 2001; 107: 881–891. https://doi.org/10.1016/S0092-8674(01)00611-0 PMID: 11779464
3. Shen X, Ellis RE, Lee K, Liu CY, Yang K, Solomon A, et al. Complementary signaling pathways regulate the unfolded protein response and are required for C. elegans development. Cell. 2001; 107: 893–903. https://doi.org/10.1016/S0092-8674(01)00612-2 PMID: 11779465
4. Calfon M, Zeng H, Urano F, Till JH, Hubbard SR, Harding HP, et al. IRE1 couples endoplasmic reticulum load to secretory capacity by processing the XBP-1 mRNA. Nature. 2002; 415: 92–96. https://doi.org/10.1038/415092a PMID: 11780124
5. Lee A-H, Iwakoshi NN, Glimcher LH. XBP-1 Regulates a Subset of Endoplasmic Reticulum Resident Chaperone Genes in the Unfolded Protein Response. Mol Cell Biol. 2003; 23: 7448–7459. https://doi.org/10.1128/MCB.23.21.7448-7459.2003 PMID: 14559994

6. Acosta-Alvear D, Zhou Y, Blais A, Tsikitis M, Lents NH, Arias C, et al. XBP1 controls diverse cell type- and condition-specific transcriptional regulatory networks. Mol Cell. 2007; 27: 53–66. https://doi.org/10.1016/j.molcel.2007.06.011 PMID: 17612490
7. Hollien J, Lin JH, Li H, Stevens N, Walter P, Weissman JS. Regulated Ire1-dependent decay of messenger RNAs in mammalian cells. J Cell Biol. 2009; 186: 323–31. https://doi.org/10.1083/jcb.200903014 PMID: 19651891
8. Ghosh R, Wang L, Wang ES, Perera BGK, Igbaria A, Morita S, et al. Allosteric inhibition of the IRE1α RNase preserves cell viability and function during endoplasmic reticulum stress. Cell. 2014; 158: 534–48. https://doi.org/10.1016/j.cell.2014.07.002 PMID: 25018104
9. Han D, Lerner AG, Vande Walle L, Upton JP, Xu W, Hagen A, et al. IRE1α Kinase Activation Modes Control Alternate Endoribonuclease Outputs to Determine Divergent Cell Fates. Cell. Elsevier Ltd; 2009; 138: 562–575. https://doi.org/10.1016/j.cell.2009.07.017 PMID: 19665977
10. Lerner AG, Upton J-P, Praveen PVK, Ghosh R, Nakagawa Y, Igbaria A, et al. IRE1α induces thioredoxin-interacting protein to activate the NLRP3 inflammasome and promote programmed cell death under irremediable ER stress. Cell Metab. 2012; 16: 250–64. https://doi.org/10.1016/j.cmet.2012.07.007 PMID: 22883233
11. Oakes SA, Papa FR. The Role of Endoplasmic Reticulum Stress in Human Pathology. Annu Rev Pathol Mech Dis. 2015; 10: 173–194. https://doi.org/10.1146/annurev-pathol-012513-104649 PMID: 25387057
12. King TE, Pardo A, Selman M. Idiopathic pulmonary fibrosis. Lancet (London, England). 2011; 378: 1949–61. https://doi.org/10.1016/S0140-6736(11)60052-4
13. Thomas AQ, Lane K, Phillips J, Prince M, Markin C, Speer M, et al. Heterozygosity for a surfactant protein C gene mutation associated with usual interstitial pneumonitis and cellular nonspecific interstitial pneumonitis in one kindred. Am J Respir Crit Care Med. 2002; 165: 1322–8. https://doi.org/10.1164/rccm.200112-123OC PMID: 11991887
14. Mulugeta S, Nguyen V, Russo SJ, Muniswamy M, Beers MF. A surfactant protein C precursor protein BRICHOS domain mutation causes endoplasmic reticulum stress, proteasome dysfunction, and caspase 3 activation. Am J Respir Cell Mol Biol. 2005; 32: 521–530. https://doi.org/10.1165/rcmb.2005-0009OC PMID: 15778495
15. Lawson WE, Cheng D-S, Degryse AL, Tanjore H, Polosukhin V V, Xu XC, et al. Endoplasmic reticulum stress enhances fibrotic remodeling in the lungs. Proc Natl Acad Sci U S A. 2011; 108: 10562–7. https://doi.org/10.1073/pnas.1107559108 PMID: 21670280
16. Wei ML. Hermansky-Pudlak syndrome: a disease of protein trafficking and organelle function. Pigment cell Res. 2006; 19: 19–42. https://doi.org/10.1111/j.1600-0749.2005.00289.x PMID: 16420244
17. Mahavadi P, Korfei M, Henneke I, Liebisch G, Schmitz G, Gochuico BR, et al. Epithelial stress and apoptosis underlie Hermansky-Pudlak syndrome-associated interstitial pneumonia. Am J Respir Crit Care Med. 2010; 182: 207–19. https://doi.org/10.1164/rccm.200909-1414OC PMID: 20378731
18. Korfei M, Ruppert C, Mahavadi P, Henneke I, Markart P, Koch M, et al. Epithelial Endoplasmic Reticulum Stress and Apoptosis in Sporadic Idiopathic Pulmonary Fibrosis. Am J Respir Crit Care Med. 2008; 178: 838–846. https://doi.org/10.1164/rccm.200802-313OC PMID: 18635891
19. Lawson WE, Crossno PF, Polosukhin V V, Roldan J, Cheng D-S, Lane KB, et al. Endoplasmic reticulum stress in alveolar epithelial cells is prominent in IPF: association with altered surfactant protein processing and herpesvirus infection. Am J Physiol Lung Cell Mol Physiol. 2008; 294: L1119–26. https://doi.org/10.1152/ajplung.00382.2007 PMID: 18390830
20. Jorgensen E, Stinson A, Shan L, Yang J, Gietl D, Albino AP. Cigarette smoke induces endoplasmic reticulum stress and the unfolded protein response in normal and malignant human lung cells. BMC Cancer. 2008; 8: 1–30. https://doi.org/10.1186/1471-2407-8-1
21. Somborac-Bacura A, van der Toorn M, Franciosi L, Slebos D-J, Zanic-Grubisic T, Bischoff R, et al. Cigarette smoke induces endoplasmic reticulum stress response and proteasomal dysfunction in human alveolar epithelial cells. Exp Physiol. 2013; 98: 316–25. https://doi.org/10.1113/expphysiol.2012.067249 PMID: 22848082
22. Hsu H-S, Liu C-C, Lin J-H, Hsu T-W, Hsu J-W, Su K, et al. Involvement of ER stress, PI3K/AKT activation, and lung fibroblast proliferation in bleomycin-induced pulmonary fibrosis. Sci Rep. Springer US; 2017; 7: 14272. https://doi.org/10.1038/s41598-017-14612-5 PMID: 29079731
23. Wang L, Perera BGK, Hari SB, Bhhatarai B, Backes BJ, Seeliger MA, et al. Divergent allosteric control of the IRE1α endoribonuclease using kinase inhibitors. Nat Chem Biol. 2012; 8: 982–989. https://doi.org/10.1038/nchembio.1094 PMID: 23086298
24. Maly DJ, Papa FR. Druggable sensors of the unfolded protein response. Nat Chem Biol. Nature Publishing Group; 2014; 10: 892–901. https://doi.org/10.1038/nchembio.1664 PMID: 25325700

25. Feldman HC, Tong M, Wang L, Meza-Acevedo R, Gobillot TA, Lebedev I, et al. Structural and Functional Analysis of the Allosteric Inhibition of IRE1α with ATP-Competitive Ligands. ACS Chem Biol. 2016; 11: 2195–2205. https://doi.org/10.1021/acschembio.5b00940 PMID: 27227314

26. Morita S, Villalta SA, Feldman HC, Register AC, Rosenthal W, Hoffmann-Petersen IT, et al. Targeting ABL-IRE1α Signaling Spares ER-Stressed Pancreatic β Cells to Reverse Autoimmune Diabetes. Cell Metab. Elsevier; 2017; 25: 883–897.e8. https://doi.org/10.1016/j.cmet.2017.03.018 PMID: 28380378

27. Papandreou I, Denko NC, Olson M, Van Melckebeke H, Lust S, Tam A, et al. Identification of an Ire1alpha endonuclease specific inhibitor with cytotoxic activity against human multiple myeloma. Blood. 2011; 117: 1311–4. https://doi.org/10.1182/blood-2010-08-303099 PMID: 21081713

28. McQualter JL, Yuen K, Williams B, Bertoncello I. Evidence of an epithelial stem/progenitor cell hierarchy in the adult mouse lung. Proc Natl Acad Sci U S A. 2010; 107: 1414–9. https://doi.org/10.1073/pnas.0909207107 PMID: 20080639

29. Chapman HA, Li X, Alexander JP, Brumwell A, Lorizio W, Tan K, et al. Integrin α6β4 identifies an adult distal lung epithelial population with regenerative potential in mice. J Clin Invest. 2011; 121: 2855–62. https://doi.org/10.1172/JCI57673 PMID: 21701069

30. Wolters PJ, Blackwell TS, Eickelberg O, Loyd JE, Kaminski N, Jenkins G, et al. Time for a change: is idiopathic pulmonary fibrosis still idiopathic and only fibrotic? Lancet Respir Med. Elsevier Ltd; 2018; 6: 154–160. https://doi.org/10.1016/S2213-2600(18)30007-9 PMID: 29413083

31. Junqueira LCU, Bignolas G, Brentani RR. Picrosirius staining plus polarization microscopy, a specific method for collagen detection in tissue sections. Histochem J. 1979; 11: 447–455. https://doi.org/10.1007/BF01002772 PMID: 91593

32. Axten JM, Medina JR, Feng Y, Shu A, Romeril SP, Grant SW, et al. Discovery of 7-methyl-5-(1-{[3-(trifluoromethyl)phenyl]acetyl}-2,3-dihydro-1H-indol-5-yl)-7H-pyrrolo[2,3-d]pyrimidin-4-amine (GSK2606414), a potent and selective first-in-class inhibitor of protein kinase R (PKR)-like endoplasmic reticulum kinase (PERK). J Med Chem. 2012; 55: 7193–207. https://doi.org/10.1021/jm300713s PMID: 22827572

33. Moreno J a, Halliday M, Molloy C, Radford H, Verity N, Axten JM, et al. Oral treatment targeting the unfolded protein response prevents neurodegeneration and clinical disease in prion-infected mice. Sci Transl Med. 2013; 5: 206ra138. https://doi.org/10.1126/scitranslmed.3006767 PMID: 24107777

34. Moore BB, Hogaboam CM. Murine models of pulmonary fibrosis. Am J Physiol Lung Cell Mol Physiol. 2008; 294: L152–60. https://doi.org/10.1152/ajplung.00313.2007 PMID: 17993587

35. Harrington PE, Biswas K, Malwitz D, Tasker AS, Mohr C, Andrews KL, et al. Unfolded Protein Response in Cancer: IRE1α Inhibition by Selective Kinase Ligands Does Not Impair Tumor Cell Viability. ACS Med Chem Lett. 2015; 6: 68–72. https://doi.org/10.1021/ml500315b PMID: 25589933

36. Burman A, Kropski JA, Calvi CL, Serezani AP, Pascoalino BD, Han W, et al. Localized hypoxia links ER stress to lung fibrosis through induction of C/EBP homologous protein. JCI insight. 2018; 3. https://doi.org/10.1172/jci.insight.99543 PMID: 30135303

37. Heindryckx F, Binet F, Ponticos M, Rombouts K, Lau J, Kreuger J, et al. Endoplasmic reticulum stress enhances fibrosis through IRE1α-mediated degradation of miR-150 and XBP-1 splicing. EMBO Mol Med. 2016; 8: 729–44. https://doi.org/10.15252/emmm.201505925 PMID: 27226027

38. Collard HR, Tino G, Noble PW, Shreve MA, Michaels M, Carlson B, et al. Patient experiences with pulmonary fibrosis. Respir Med. 2007; 101: 1350–1354. https://doi.org/10.1016/j.rmed.2006.10.002 PMID: 17107778

39. Raghu G, Collard HR, Egan JJ, Martinez FJ, Behr J, Brown KK, et al. An official ATS/ERS/JRS/ALAT statement: idiopathic pulmonary fibrosis: evidence-based guidelines for diagnosis and management. Am J Respir Crit Care Med. 2011; 183: 788–824. https://doi.org/10.1164/rccm.2009-040GL PMID: 21471066

40. Watkin LB, Jessen B, Wiszniewski W, Vece TJ, Jan M, Sha Y, et al. COPA mutations impair ER-Golgi transport and cause hereditary autoimmune-mediated lung disease and arthritis. Nat Genet. Nature Publishing Group; 2015; 47: 654–60. https://doi.org/10.1038/ng.3279 PMID: 25894502

41. Kamp DW, Liu G, Cheresh P, Kim S-J, Mueller A, Lam AP, et al. Asbestos-induced alveolar epithelial cell apoptosis. The role of endoplasmic reticulum stress response. Am J Respir Cell Mol Biol. 2013; 49: 892–901. https://doi.org/10.1165/rcmb.2013-0053OC PMID: 23885834

42. Vaughan A, Vaughan A, Brumwell A, Chapman H. Lung Epithelial Cell Prep. Protoc Exch. Nature Publishing Group; 2015; https://doi.org/10.1038/protex.2015.017